Antitumor Activity of Cell-Permeable p18^{INK4c} With Enhanced Membrane and Tissue Penetration

Junghee Lim[1,2], Jungeun Kim[1], Tam Duong[3], Guewha Lee[1], Junghee Kim[1], Jina Yoon[1], Jaetaek Kim[4], Hyuncheol Kim[2], H Earl Ruley[5], Wael El-Rifai[6,7] and Daewoong Jo[1,3,6]

[1]ProCell R&D Institute, ProCell Therapeutics, Inc., Seoul, Korea; [2]Interdisciplinary Program of Integrated Biotechnology, Sogang University, Seoul, Korea; [3]Department of Biomedical Sciences, Chonnam National University Medical School, Kwangju, Korea; [4]Department of Internal Medicine, College of Medicine, Chung-Ang University, Seoul, Korea; [5]Department of Pathology, Microbiology and Immunology, Vanderbilt University School of Medicine, Nashville, Tennessee, USA; [6]Department of Surgery, Vanderbilt University School of Medicine, Nashville, Tennessee, USA; [7]Department of Cancer Biology, Vanderbilt University School of Medicine, Nashville, Tennessee, USA

Practical methods to deliver proteins systemically in animals have been hampered by poor tissue penetration and inefficient cytoplasmic localization of internalized proteins. We therefore pursued the development of improved macromolecule transduction domains (MTDs) and tested their ability to deliver therapeutically active p18^{INK4c}. MTD103 was identified from a screen of 1,500 signal peptides; tested for the ability to promote protein uptake by cells and tissues; and analyzed with regard to the mechanism of protein uptake and the delivery of biologically active p18^{INK4c} into cancer cells. The therapeutic potential of cell-permeable MTD103p18^{INK4c} (CP-p18^{INK4c}) was tested in the HCT116 tumor xenograft model. MTD103p18^{INK4c} appeared to traverse plasma membranes directly, was transferred from cell-to-cell and was therapeutically effective against cancer xenografts, inhibiting tumor growth by 86–98% after 5 weeks ($P < 0.05$). The therapeutic responses to CP-p18^{INK4c} were accompanied by high levels of apoptosis in tumor cells. In addition to enhancing systemic delivery of CP-p18^{INK4c} to normal tissues and cancer xenografts, the MTD103 sequence delayed protein clearance from the blood, liver and spleen. These results demonstrate that macromolecule intracellular transduction technology (MITT), enabled by MTDs, may provide novel protein therapies against cancer and other diseases.

Received 2 March 2012; accepted 19 April 2012; advance online publication 22 May 2012. doi:10.1038/mt.2012.102

INTRODUCTION

The mammalian cell cycle is regulated by the sequential activation of cyclin-dependent kinases (CDKs) whose activities are restrained by physical interactions with CDK inhibitors (CKIs).[1,2] These controls integrate the cell cycle with extracellular signals required for cell growth, differentiation, and survival and provide check-points to guard against unscheduled cell proliferation and maintain genome integrity. For example, transition through the first gap phase (G_1) and entry into S phase is orchestrated initially by CDKs 4 and 6 in association with their activating subunits, the D type cyclins, and negatively regulated by members of the inhibitor of kinase 4 (INK4; p16^{INK4a}, p15^{INK4b}, p18^{INK4c}, and p19^{INK4d}) CKI proteins and subsequently by CDK2/Cyclin E, restrained by the Cip/Kip CKIs (p21$^{Waf1/Cip1}$, p27^{Kip1}, and p57^{Kip2}). In addition, several of the Cip/Kip CKIs stimulate the assembly and activity of the Cyclin D-CDK4/6 complexes with which they associate; these interactions then divert the Cip/Kip proteins from suppressing Cyclin E-CDK2 activity.[1,2]

Although not required for mammalian cell proliferation, the G_1 CDKs play critical roles in the development and maintenance of specialized cell types, including erythroid progenitors, cardiomyocytes and pancreatic β cells.[1] Moreover, the activities of the G_1 CDKs are frequently elevated in human tumors by a variety of mechanisms, including Cyclin D overexpression, activating mutations in CDK4, and loss-of-function mutations involving INK4 and Cip/Kip CKIs.[1] The latter rank among the most common tumor suppressor gene mutations in human cancer. Finally, in some settings CDK4 activity is required for malignant transformation[3–6] and allows tumor cells to tolerate the otherwise lethal effects of an activated oncogene.[7] Such considerations establish the G_1 CDKs as potential targets for anticancer drug development,[8] and provide the rationale for ongoing clinical trials of several CDK4/6 inhibitors.[8,9]

A common problem with small-molecule kinase inhibitors is the potential for off-target drug interactions.[8] To address this issue, we have investigated the use of macromolecule intracellular transduction technologies (MITTs) to deliver biologically active CKIs, specifically p18^{INK4c}, into cultured tumor cells and animal tissues. In principle, cell-permeable p18^{INK4c} proteins provide a means to inhibit CDKs 4 and 6 specifically, establishing if not a protein-based cancer therapy, then a reference against which to evaluate candidate small-molecule CDK inhibitors. Moreover, by modulating the differentiation and/or renewal of stem cells with specific requirements for CDKs 4 and 6 activity (*e.g.*, erythroid progenitors, cardiomyocytes, and pancreatic β cells), cell-permeable p18^{INK4c} could have therapeutic applications in such areas as stem cell cytoprotection and regenerative medicine.

Intracellular macromolecule transduction exploits the ability of specific basic, amphipathic and hydrophobic (or amphipathic

Correspondence: *Daewoong Jo, Department of Surgery, Vanderbilt University School of Medicine, 1255 MRB IV, 2215B Garland Avenue, Nashville, Tennessee 37232, USA. E-mail: dae-woong.jo@vanderbilt.edu*

depending on cargo) protein sequences to enhance the uptake of proteins and other macromolecules by mammalian cells.[10,11] Although protein transduction has been widely used as an experimental tool, systemic delivery of proteins in animals has proven difficult due to inefficient cytoplasmic delivery of internalized proteins and poor tissue penetration. This is particularly true for the cationic protein transduction domains (PTDs, *e.g.*, HIV Tat, Hph-1, Antennapedia (Ant), polyarginine, etc.) where the predominant mechanisms of protein uptake—absorptive endocytosis and macropinocytosis—sequester significant amounts of protein into membrane-bound and endosomal compartments, thus limiting protein bioavailability.[10,11] Greater success has been reported for a sequence (designated membrane translocating sequence, or MTS) derived from the hydrophobic signal peptide of fibroblast growth factor 4 (FGF4). The MTS has been used to deliver biologically active peptides and proteins systemically in animals (in particular to liver, lung, pancreas, and lymphoid tissues), with dramatic protection against lethal inflammatory disease[12–17] and pulmonary metastases.[18]

Peptide MTS-containing cargos appear to enter cells directly by penetrating the plasma membrane.[19,20] In principle, this is expected to reduce endosomal sequestration and enhance cell-to-cell transfer within tissues, thus increasing *in vivo* bioavailability of MTS- as compared to PTD-containing cargos. However, the overall potential of hydrophobic sequences to enhance protein delivery and uptake in tissues cannot be assessed until a greater variety of cargos have been tested, particularly since the effectiveness of the FGF4 MTS varies greatly, depending on the protein cargo. For example, the Cre DNA site-specific recombinase, a basic protein, has a low but intrinsic ability to enter cells which is greatly increased by the addition of a 6xHis affinity purification tag and SV40 nuclear localization sequence (NLS).[21] Both elements appeared to stimulate endocytic uptake and thus functioned as cationic PTDs. Transduction of 6xHis-NLS-Cre was only modestly enhanced by the HIV Tat PTD and then only at lower protein concentrations. All other transduction sequences tested, including the FGF4 MTS, inhibited Cre uptake, as did HIV Tat at higher protein concentrations. In short, protein uptake depends on multiple, and potentially competing, mechanisms and is heavily influenced by the cargo and such nonspecific factors as protein concentration, aggregation, and solubility.[10–11,22]

In the present study, we developed several new hydrophobic sequences (designated macromolecule transduction domains, or MTDs) that enhance protein uptake by cultured cells and animal tissues at levels greater than or equal to the FGF4 sequence or cationic sequences from HIV-1 Tat, human Hph-1 (Hph) and *Drosophila* Ant. We investigated the ability of one of these sequences, MTD103, to enhance intracellular delivery of biologically active p18^{INK4c} *in vitro* and *in vivo*, and investigated the mechanism of protein uptake. The 6xHis tagged MTD103-p18^{INK4c} recombinant protein (HM_{103}p18) appeared to traverse membranes directly, was transferred from cell-to-cell and was therapeutically effective in a mouse xenograft tumor model.

RESULTS

Development of a cell-permeable p18 ^{INK4c} tumor suppressor

The hydrophobic MTS from the signal peptide of FGF4 has been previously used to deliver protein cargos into cultured cells and animals. We identified seven peptides with activities greater than or comparable to the FGF4 MTS that were selected for further modification (**Supplementary Table S1**) and promoted uptake of FITC-EGFP by cultured RAW264.7 cells (**Supplementary Figure S1a**) and systemic delivery to various tissues in mice (**Supplementary Figure S1b**) at levels comparable to, if not greater than, the FGF4 MTS (M_m).

One of the seven peptides, MTD103, and several cationic PTDs (**Supplementary Tables S2** and **S3** and **Figure S2a**) were tested for their ability to enhance the uptake of recombinant p18^{INK4c} protein by mammalian cells. Hp18 consists of an amino terminal 6x histidine tag and NLS from SV40 large T antigen appended to the human p18^{INK4c} sequence (residues 2-168). HM_{103}p18, HTatp18, HHphp18 and HAntp18 are identical to Hp18 but contain the hydrophobic MTD103 sequence or PTDs from HIV Tat, human Hph-1 and *Drosophila* Ant, respectively. Each protein was expressed in *Escherichia coli* (**Supplementary Figure S2b**), purified under denaturing conditions and refolded, with yields of soluble protein ranging from 2 to 30 mg/l (**Supplementary Figure S2a**).

In a pilot study to examine protein uptake HM_{103}p18 entered RAW264.7 cells efficiently (**Supplementary Figure S3a,b**), unlike Hp18, confirming the ability of the MTD103 sequence to promote protein uptake and establishing Hp18 as a negative control for protein transductions studies involving p18^{INK4c} cargos. We next compared protein transduction mediated by MTD103 to that of sequences derived from Tat, Hph, and Ant. HM_{103}p18 displayed the highest levels of protein in cultured RAW264.7 cells (**Figure 1a**) and peripheral blood leukocytes (**Figure 1b**). Cell-associated fluorescence appeared to be intracellular since the signal was resistant to washing and protease treatment and was enhanced by MTD103 and to a lesser extent by the Tat, Hph, and Ant sequences. We also examined the distribution of native proteins in the serum, liver, and spleen by immunoblotting after intraperitoneal injection (**Figure 1c**). The highest plasma levels were observed in mice injected with HM_{103}p18, illustrating the ability of MTD103 to deliver proteins into circulation. Protein levels in plasma declined more rapidly than tissue-associated protein (**Figure 1c**). Much of decline appeared to reflect clearance from the blood rather than degradation, since recombinant proteins were stable when incubated with plasma *in vitro*. The distribution of proteins in liver and spleen sections was consistent with hematogeneous delivery (**Figure 1d**).

MTD103-mediated protein uptake

Since MTD103 outperformed the other transduction domains tested, we next investigated the mechanism of MTD103-mediated protein uptake. The hydrophobic FGF4 MTS is thought to enter cells directly by penetrating the plasma membrane.[19,20] However, endocytosis may mediate bulk entry of some proteins, *e.g.*, Cre recombinase,[21] regardless of whether they carry a hydrophobic MTS. We therefore investigated the mechanism of fluorescein isothiocyanate (FITC)-labeled HM_{103}p18 uptake in cultured cells.

Several lines of evidence suggest endocytosis was not the major route of entry by HM_{103}p18. In particular, uptake was unaffected by treatment of cells with proteases (**Supplementary Figure S4a**), microtubule inhibitors (**Supplementary Figure S4b**), or the ATP-depleting agent, antimycin (**Supplementary Figure S4c**).

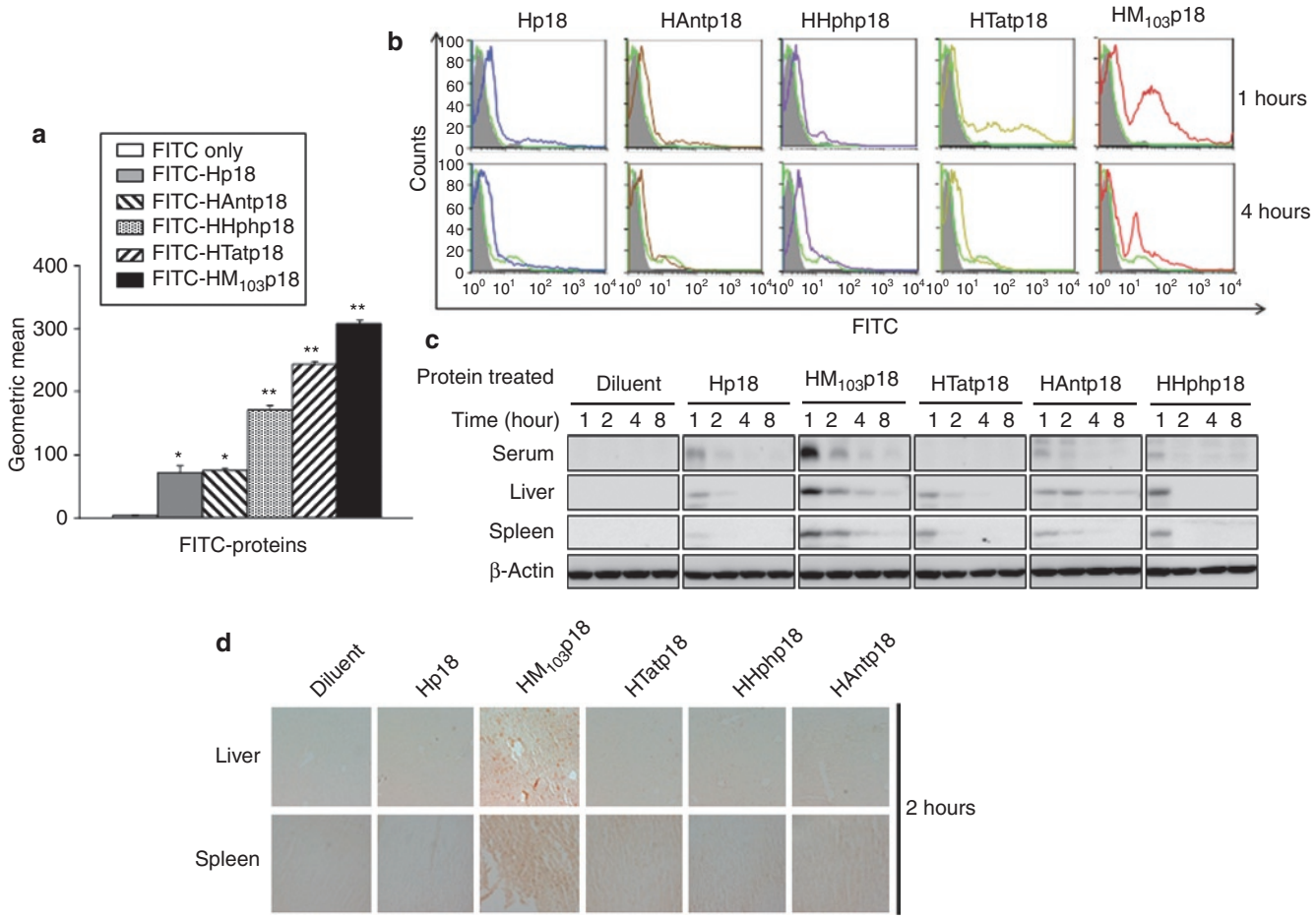

Figure 1 Macromolecule transduction domain (MTD)- and protein transduction domain (PTD)-mediated protein delivery into cells and tissues. (**a**) Uptake of fluorescein isothiocyanate (FITC)-labeled proteins by RAW264.7 cells. Cells were exposed to the indicated proteins (10 µmol/l) for 1 hour, treated to remove cell-associated but noninternalized protein and analyzed by flow cytometry. The geometric means of FITC fluorescent peaks are plotted. (**b**) Uptake of FITC-labeled proteins by white blood cells. FACS profiles of WBC prepared from mice after intraperitoneal (i.p.) injection (300 µg/head) [FITC only (shaded); Hp18 (light green) and the indicated proteins (other colors)]. (**c**) Western blot analysis of proteins in serum, liver, and spleen. (**d**) Liver and tissue distribution of recombinant proteins. Tissue sections from mice were prepared 2 hours postinjection and immunostained with anti-p18INK4c antibody.

Conversely, HM_{103}p18 uptake was blocked by conditions affecting membrane fluidity (temperature) and integrity (EDTA) (Figure 2a,b). Finally, MTD103 enhanced the delivery of p18INK4c cargo by over fourfold into artificial phospholipid/cholesterol vesicles (Figure 2c). Moreover, we also tested whether cells containing HM_{103}p18 could transfer the protein to neighboring cells. For this, cells transduced with FITC-HM_{103}p18 (green) were mixed with CD14-labeled cells (red) and cell-to-cell protein transfer was assessed by flow cytometry, scoring for CD14/FITC double-positive cells. Efficient cell-to-cell transfer of HM_{103}p18, but not Hp18 (Figure 2d), suggests MTD103 containing proteins are capable of bidirectional passage across the plasma membrane.

Biological activities of cell-permeable p18INK4c

The cell-permeable p18INK4c appeared to be biologically active, as HM_{103}p18-treated cells expressed lower levels of phosphorylated retinoblastoma tumor suppressor (Rb; reduced by 90%) and higher levels of p21 (7.6-fold); and higher levels of phosphorylated p53 and ATM (6–10-fold), as compared to Hp18-treated cells (Figure 3a).

The p18INK4c CKI is specific for complexes between D type Cyclins and either CDK4 or CDK6 (ref. 23). We measured the CKI activity of recombinant HM_{103}p18 and Hp18 proteins with an *in vitro* kinase assay against Rb substrate. Both proteins had similar IC_{50}s against CDK6, which improved (from 4 µmol/l to <250 nmol/l) after the refolding step in their preparation. However, the intracellular activity of the cell-permeable HM_{103}p18 protein was considerably greater than that of the control Hp18 protein as assessed either by the inhibition of Rb phosphorylation or by secondary effects on p53 phosphorylation, p21 expression and ATM phosphorylation (Figure 3a). This experiment also examined five other recombinant proteins: HM_{101}p18 is identical to HM_{103}p18 but utilized the MTD101 sequence (**Supplementary Table S1**); Hp18M_{101} and Hp18M_{103} have MTD sequences positioned on the carboxyl- rather than amino terminal ends of the protein; and HM_{103}p18M_{103} and HM_{101}p18M_{101} each contain an additional MTD sequence at the carboxyl-terminal end of the protein (**Supplementary Table S3** and **Supplementary Figure S5**). HM_{103}p18 was a considerably more efficient inducer of apoptosis than control proteins in HCT116 cancer cells, as assessed either by annexin V staining or by Caspase-3

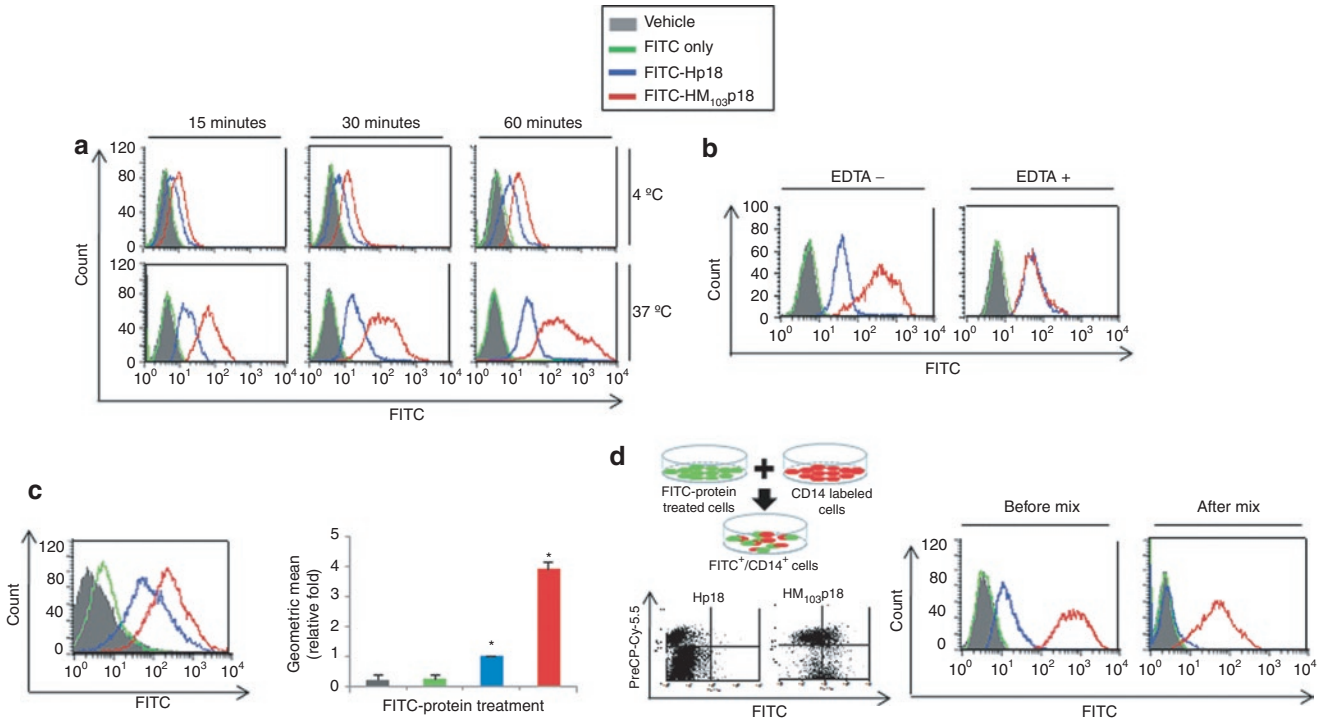

Figure 2 Mechanism of MTD103-mediated protein uptake. (**a**) Temperature-dependence of MTD103-stimulated protein uptake. RAW264.7 cells were exposed for the indicated times to 10 µmol/l HM_{103}p18 (red), 10 µmol/l Hp18 (blue), an equimolar concentration of unconjugated fluorescein isothiocyanate (FITC) (FITC only, green) or were untreated (shaded), were washed and treated with proteinase K to remove cell-associated but noninternalized protein and analyzed by flow cytometry. (**b**) EDTA suppresses MTD103-stimulated protein uptake. RAW264.7 cells (shaded) were treated or untreated with 100 mmol/l EDTA for 3 hours were exposed for one hour to 10 µmol/l HM_{103}p18 (red), 10 µmol/l Hp18 (blue), FITC only (green), were processed as before to remove noninternalized protein and were analyzed by flow cytometry. (**c**) MTD103 stimulates protein uptake into artificial lipid vesicles. Chloresterol/phosphatidylcholine vesicles (shaded) were treated with FITC alone (green) or with 10 µmol/l Hp18 (blue) or 10 µmol/l HM_{103}p18 (red), were processed as before to remove noninternalized protein and were analyzed by flow cytometry. The geometric means of FITC fluorescent peaks (left panel) were plotted (right panel). (**d**) Cell-to-cell transfer of cell-permeable p18INK4c. RAW264.7 cells were exposed to 10 µmol/l FITC-Hp18 or FITC-HM_{103}p18 and after 2 hours the cells were processed to remove noninternalized protein, were mixed with cells stained with Cy5.5 labeled anti-CD14 antibody, and analyzed by flow cytometry. The left panel shows a mixture of double negative cells (cells exposed to FITC-Hp18 that did not incorporate the protein) and single-positive Cy5.5-labeled cells; whereas, second panel from the left contains FITC-Cy5.5 double-positive cells generated by the transfer of FITC-HM_{103}p18 to Cy5.5-labeled cells and the remaining FITC and Cy5.5 single-positive cells. The right two panels show FITC fluorescence profiles of cell populations before mixing (coded as before) and 1 hour after the same cells were mixed with Cy5.5-labeled cells. MTD, macromolecule transduction domain.

activation (**Figure 3b** and **Supplementary Figure S6**). In addition, no changes in annexin V staining or Caspase-3 activity were observed in untransformed RAW264.7 and NIH3T3 cells treated with CP-p18INK4c. We conclude that differences in the biological activities of HM_{103}p18 or HM_{101}p18 as compared to Hp18 are due to differences in protein uptake mediated by the MTD sequences.

Systemic delivery of cell-permeable p18INK4c

High levels of HM_{103}p18 were observed in ~60% of peripheral white blood cells after 1 hour of intraperitoneal injection of FITC-labeled HM_{103}p18 (**Figure 4a**). Similar levels of protein uptake were observed in both leukocytes and lymphocytes; however, neutrophils contained relatively low levels of the protein, suggesting phagocytic cells are not intrinsically more active at internalizing recombinant p18INK4c proteins (**Figure 4b**). HM_{103}p18 was also delivered to the spleen and liver with similar kinetics, as assessed by either immunostaining (**Figure 4c**) or western blot analysis (**Figure 4d**) and persisted for several hours, declining with a half-life of ~1 hour (**Figure 4d**). By contrast, proteins lacking the MTD sequence failed to accumulate in any the blood cells or tissues analyzed (**Figure 4**). In addition, Intraperitoneally administrated Q-dot-labeled recombinant HM_{103}p18 was delivered to major organs such as liver and lung by fusing to only MTD (MTD103), but not PTD (HIV Tat) (**Supplementary Figure S7**, left panel). Intravenously injected HM_{103}p18 was sufficiently delivered *in vivo*, distributed to solid tumors, persisted from 6 to 24 hours (**Supplementary Figure S7**, left panel). These results demonstrate the ability of MTD103 to deliver a biologically active p18INK4c fusion protein to multiple cells and tissues.

Cell-permeable p18INK4c suppresses the growth of human tumor xenografts

The growth of xenografted tumors in HM_{103}p18-treated mice lagged significantly ($P < 0.05$) behind those in control animals during the course of the experiment over 38 days and persisted for at least 2 weeks after treatment was terminated (**Figure 5a**). Similar results were obtained in a second group of mice treated for 21 days (300 µg) and followed for a total of 42 days (**Figure 5b**). A cell-permeable EGFP protein (HM_{103}E) served as an additional negative control. Differences in tumor responses are further illustrated by comparing representative tumors excised from diluent- and

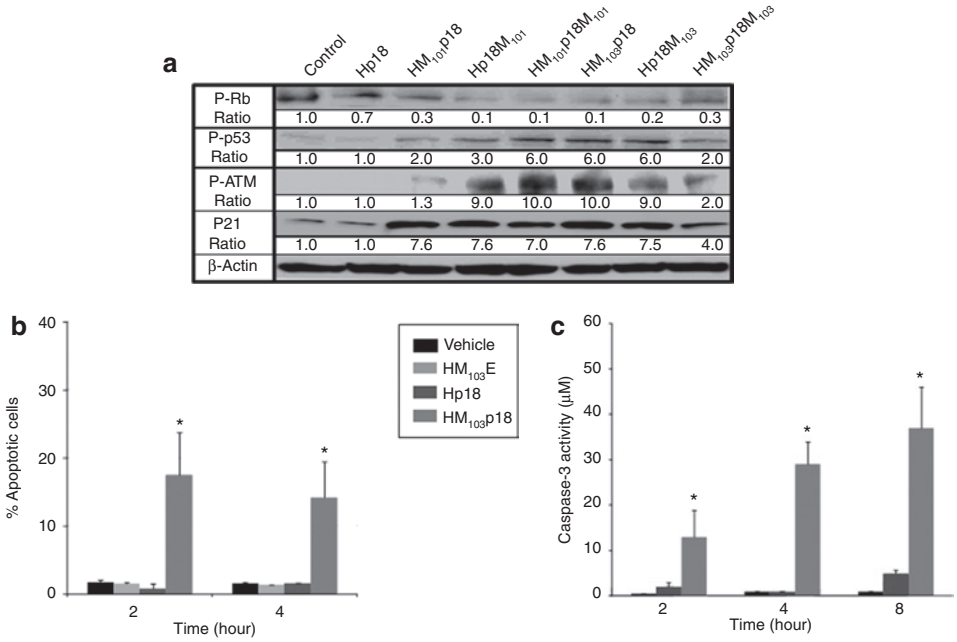

Figure 3 Cell-permeable p18INK4c induces apoptosis. (**a**) Biomarker expression. HCT116 cells were treated with the indicated proteins (10 μmol/l) for hour and cell extracts were immunoblotted with antibodies against phospho-Rb (Ser780), phospho-p53 (Ser15), phospho-ATM (Ser1981), p21Waf1/Cip1 and β-actin. (**b**) Kinetics of apoptosis induction. HCT116 cells, treated with 10 μmol/l $HM_{103}E$, Hp18, and $HM_{103}p18$ for the indicated times, were stained with fluorescein isothiocyanate (FITC)-labeled annexin V and propidium iodide and analyzed by flow cytometry. The percentage of annexin V positive cells (±SD of triplicate experiments) is plotted. *Significant differences ($P < 0.05$) between $HM_{103}p18$ as compared to vehicle, $HM_{103}E$ or Hp18 as determined by one-tailed Student's *t*-tests. (**c**) Kinetics of Caspase-3 activation. HCT116 cells were treated as before with 10 μmol/l $HM_{103}E$, Hp18, and $HM_{103}p18$. Caspase-3 assays measured production (±SD of triplicate experiments) of cleaved Caspase-3 substrate (Clonetech, Mountain View, CA) by increased absorbance at 405 nm after 1 hour at 37 °C. *Significant differences ($P < 0.05$) between $HM_{103}p18$ and other samples as determined by one-tailed Student's *t*-tests.

$HM_{103}p18$-treated mice from the first experiment (**Figure 5c**) or alternatively excised from half of the animals at the end of protein therapy in the second experiment (**Figure 5d**). The recombinant proteins were well-tolerated (**Supplementary Figure S8a,b**).

Delivery of CP-p18INK4c protein to the tumor xenografts was confirmed by immunostaining 24 hours after intravenous injection (300 μg/mouse) using antibodies against p18INK4c or the MTD103 sequence; whereas, only low levels of the Hp18 control protein were detected with anti-p18INK4c but not anti-MTD103 (**Figure 6a**). The therapeutic responses to CP-p18INK4c were accompanied by high levels of apoptosis within the tumors, as assessed by biomarker expression (**Figure 6b,c**) and by Apop Tag and TUNEL staining (**Figure 6d**). In particular, the levels of p21, activated Caspase-3, PUMA, and Bax increased in $HM_{103}p18$-treated tumors, while levels of Bcl2, XIAP, Cyclin D1, and ICAM-1 declined.

Larger tumors (~120 mm^3) also responded to protein therapy; however, tumor growth was inhibited by 70% (**Figure 7a,b**) as compared to 86–98% (**Figure 5a,b**). These data suggest that initial tumor size plays a role in the antitumorigenic effects of CP-p18INK4c. This is may reflect the fact that subcutaneous tumors are poorly vascularized, limiting the ability of cell-permeable proteins to gain access to larger tumors. Protein treatment did not affect mouse body weights (**Supplementary Figure S8c,d**).

DISCUSSION

Protein transduction approaches for systemic therapeutic delivery of proteins and peptides have been hampered due to inefficient cytoplasmic delivery of internalized proteins and poor tissue penetration.[10,11] In the present study, we identified several new hydrophobic MTDs, capable of enhancing protein uptake by cultured cells and in animal tissues. We used one of these sequences, MTD103, to deliver biologically active p18INK4c systemically in mice, and significantly inhibited tumor growth in a colon cancer xenograft model. This study is the first to describe a functional cell-permeable p18INK4c and establishes MTD103 as a potential delivery vehicle for protein-based therapeutics.

Tumor suppression using CP-p18INK4c strictly required the MTD103 sequence and inhibition of tumor growth continued for at least 2 weeks after protein therapy was terminated. The therapeutic response was accompanied by high levels of tumor cell apoptosis including the activation of pro-apoptotic pathways (p53, p21, and Caspase-3), and suppression of prosurvival proteins (Bcl2, XIAP and ICAM-1). In addition to targeting tumor cells, it is possible that the therapeutic activity of CP-p18INK4c may benefit from targeting other cells or processes (*e.g.*, angiogenesis) that influence tumor cell survival.

The antitumor activity of $HM_{103}p18$ exceeded that of previously described cell-permeable INK4 and Cip/Kip Cyclin-dependent kinase inhibitors,[24–29] all of which employed the HIV Tat PTD. Several considerations suggest the greater *in vivo* activity of $HM_{103}p18$ resulted from enhanced protein delivery mediated by MTD103 and not from some special attribute of the p18INK4c cargo as compared to other CKIs. The MTD103 enhanced bidirectional transfer of p18INK4c across the plasma membrane circumventing

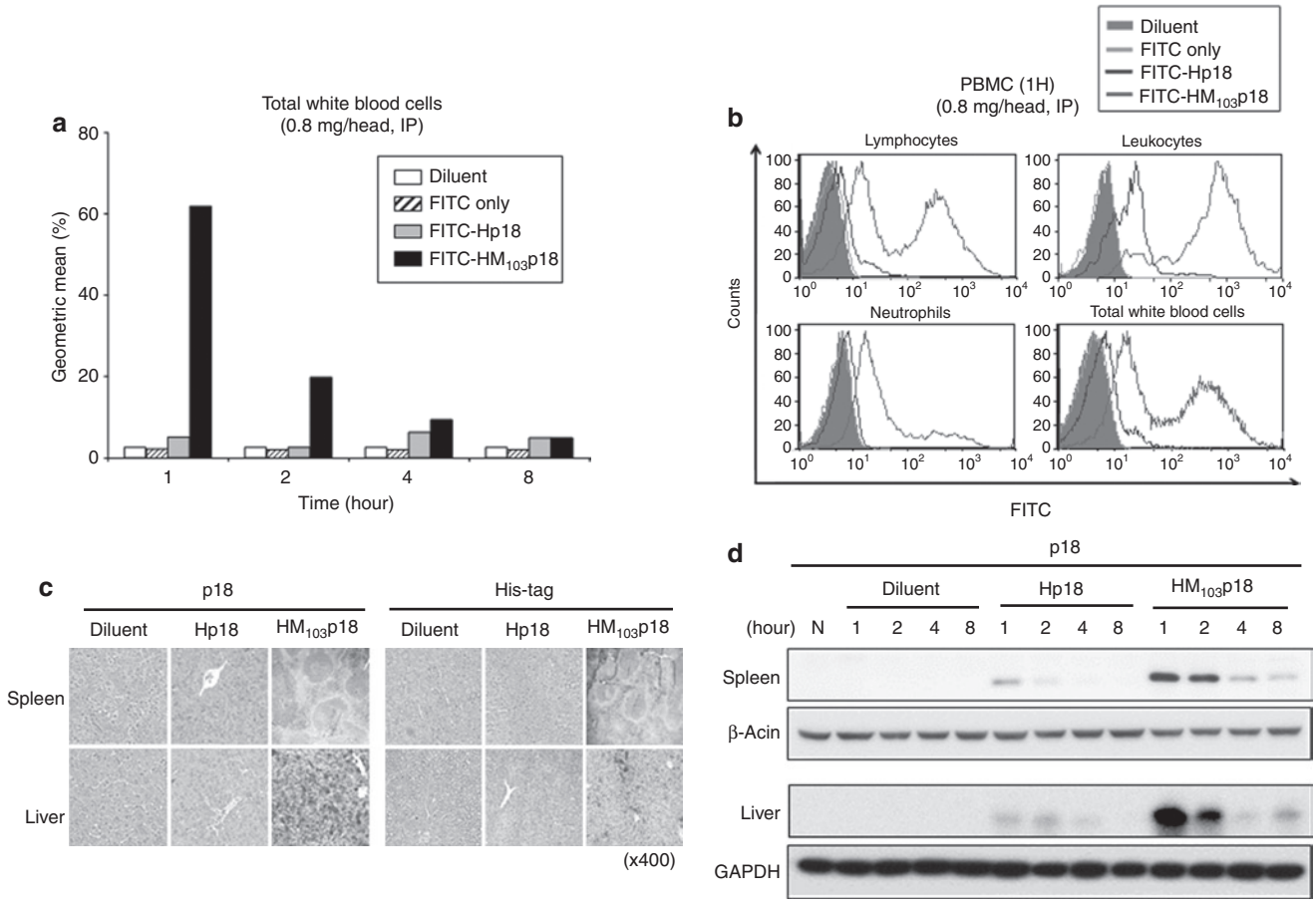

Figure 4 Systemic delivery of cell-permeable p18INK4c. (**a**) Uptake of fluorescein isothiocyanate (FITC)-labeled proteins by white blood cells. Mice were injected intraperitoneal (i.p.) with diluent, 20 µg FITC or 800 µg of FITC-Hp18, or FITC-HM_{103}p18 and at the indicated times, WBCs were analyzed by flow cytometry. The geometric means of FITC fluorescent peaks are plotted. (**b**) Uptake of FITC-labeled proteins by WBC subpopulations. The experiment was performed as in (**a**) except WBC subpopulations were analyzed after staining with phycoerythrin (PE)-conjugated antibodies to lymphocyte (B220 plus CD3), leukocyte (CD116), neutrophil (Ly6G) markers. (**c**) Tissue (spleen and liver) distribution of recombinant proteins. Paraffin-embedded issue sections were prepared from mice 2 hours postinjection (600 µg, i.p.) and immunostained with anti-p18INK4c antibody. (**d**) Persistence of Hp18 and HM_{103}p18 proteins in spleen and liver. Mice were injected with the indicated proteins as before and at the indicated times postinjection, tissue extracts were immunoblotted with antibodies against p18INK4c, β-actin, or glyceraldehyde phosphate dehyrogenase (GAPDH).

a major limitation of the cationic PTDs, whose predominant mechanisms of protein uptake—absorptive endocytosis and macropinocytosis—sequester significant amounts of protein into membrane-bound and endosomal compartments. The MTD103 sequence also extended the half-life of recombinant p18INK4c proteins *in vivo*, presumably due to enhanced stability and/or decreased plasma clearance of internalized p18INK4c as compared to extracellular protein.

MTD103 joins a growing number of hydrophobic sequences that have been used to enhance the delivery of proteins into mammalian cells. These include MTD39, MTD41, MTD52, MTD58, MTD68, and MTD101 (**Supplementary Table S1**); MTD76 and MTD77;[18] and signal sequence-derived peptides from integrin β3 and FGF4.[30,31] Sequences from the FGF4 signal peptide to deliver a nuclear import inhibitor peptide and suppressor of cytokine signaling 3 (SOCS3) protein have been used with remarkable therapeutic efficacy in animal models of acute inflammation.[12–17] Our findings in this study together with our earlier report using cell-permeable NM23 metastasis suppressor 18 highlight the potential of protein delivery approaches in cancer therapeutics.

The limited vascularization of subcutaneous tumors provides a challenging test of *in vivo* protein delivery and uptake. The widespread tissue distribution and biological activity of HM_{103}p18 against subcutaneous tumors, particularly after intraperitoneal administration, illustrates the ability of MTD-containing peptides and proteins to penetrate multiple cell and tissue barriers. Previous studies suggest the FGF4 hydrophobic MTS peptide penetrates the plasma membrane directly[19] after inserting into the membranes in a "bent" configuration with hydrophobic sequences adopting an α-helical conformation.[20] The present study provides the first evidence that a similar mechanism can mediate MTD-dependent uptake of larger protein cargos. In particular, we show that the uptake of HM_{103}p18 is sensitive to low temperature, does not require microtubule reorganization, is not enhanced by agents that disrupts the plasma membrane, and does not utilize ATP. Furthermore, HM_{103}p18 traverses artificial bilayers consisting of cholesterol and phospholipid and is capable of bidirectional movement across membranes as assessed by cell-to-cell protein transfer. Properties of MTD103 required for efficient cellular uptake and systemic delivery *in vivo* are clearly shared by a number of peptide sequences ranging from 7–10 amino

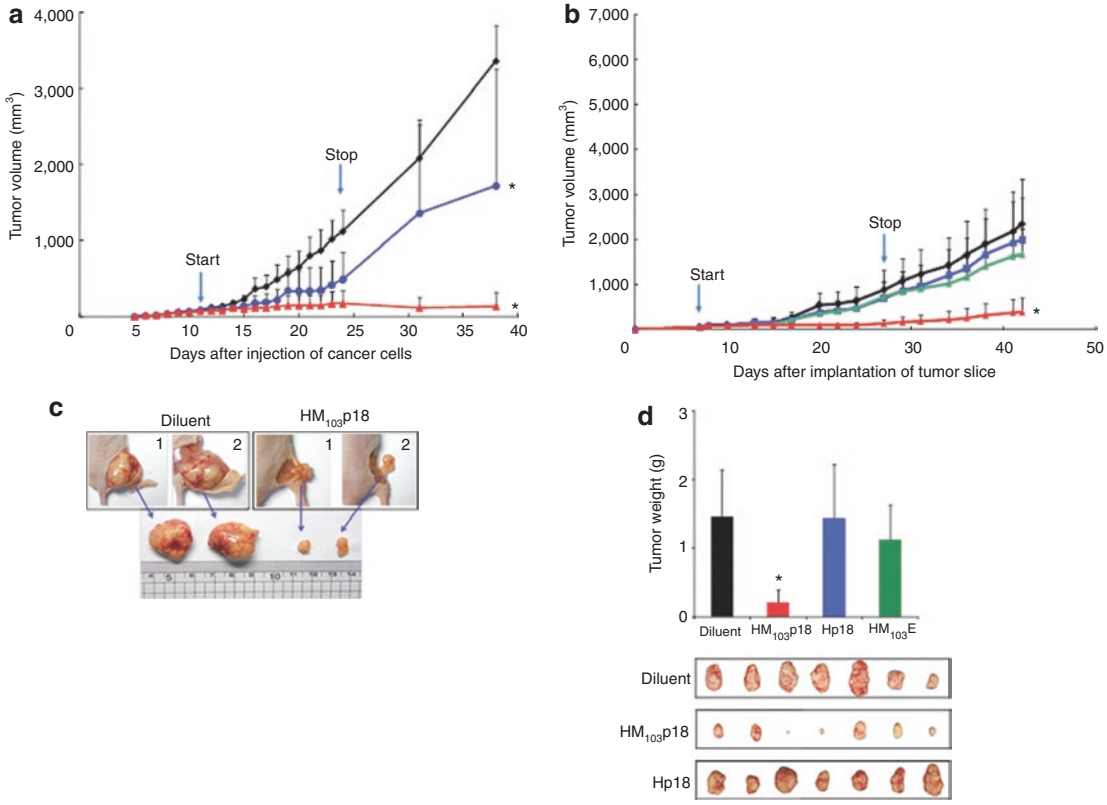

Figure 5 Cell-permeable p18^{INK4c} suppresses tumor cell growth. (**a**–**d**) Suppression of tumors induced by subcutaneous injection of HCT116 tumor cells (**a**,**c**) or HCT116 tumor explants (**b**,**d**). After tumors reached a size of ~60 mm³ (start), the mice were injected daily (i.v.) for 2–3 weeks with diluent alone (black) or with 300 µg Hp18 (blue), HM_{103}p18 (red), or HM_{103}E (green). Suppression of tumor growth persisted for at least 2 weeks after protein therapy ended (stop) after which, representative tumors from (**a**) and (**b**) were examined as shown in (**c**) and (**d**), respectively.

acids in size. However, additional studies will be required to confirm direct transfer to the cytosol and to assess the extent to which protein uptake involves other, potentially competing, mechanisms and is influenced by the cargo and such nonspecific factors as protein concentration, aggregation, and solubility.

In addition, we are currently trying to identify the optimal sequence and/or structural determinants for tissue delivery/uptake and assess potential contributions by cargo sequences. Like the FGF4 MTS,[20] MTD103 is predicted to adopt a helical conformation (**Supplementary Figure S9**). In contrast, the PTDs from Tat, Hph-1, and Ant are predicted to adopt random coils. However, any understanding of structure-activity relationships will require experimentally determined protein structures and data on a larger number of MTD sequences. While the hydrophobic MTD103 sequence was strictly required for efficient cellular uptake and systemic delivery *in vivo*, potential contributions by protein cargo sequences cannot be excluded and could be important determinants of tissue penetration and/or *in vivo* bioavailability.

The antitumor activity of cell-permeable p18^{INK4c}, although striking when compared to previous cell-permeable CKI proteins, still fell short of that reported for small-molecule CDK4/6 inhibitors, such as PD 0332991.[32] It is possible that some antitumor activities of PD 0332991 result from off-target effects; whereas, cell-permeable p18^{INK4c} is expected to have greater target selectivity and potentially lower toxicity. The IC_{50} of recombinant HM_{103}p18 as assayed by Cyclin D/CDK4-dependent Rb phosphorylation was higher than others have reported for purified p18^{INK4c} protein.[33,34] Therefore, some improvements in formulation and/or modifications of HM_{103}p18 by using different MTDs and proteins with and without His tag or NLS sequences might further enhance therapeutic activity of the protein. Finally, we expect improvements to protein refolding and solution-formulation will enhance stability, reduce aggregation, and/or increase fill-finish concentration. In conclusion, this pilot study suggests that HM_{103}p18 could have antitumor therapeutic activity as well as additional therapeutic applications by modulating the proliferation, differentiation and survival of stem cells with specific requirements for CDK4/6.

MATERIALS AND METHODS

Preparation of recombinant p18^{INK4c} fusion proteins. MTD sequences, including MTD103, were identified from a screen of 1,500 signal peptides for sequences with protein transduction activity and were subsequently modified (D. Jo *et al.*, manuscript in preparation). Coding sequences for p18^{INK4c} and EGFP fusion proteins were cloned into pET-28a(+) (Novagen, Darmstadt, Germany) from PCR-amplified DNA segments (**Supplementary Table S1**). EGFP fusion proteins included a positive control containing the MTS from FGF4 (AAVLLPVLLAAP) and an arbitrary peptide (SANVEPLERL) that served as a negative control. Hp18 consists of an amino terminal 6x histidine tag (MGSSHHHHHHSSLVPRGSH) and NLS (KKKRK) from SV40 large T antigen appended to the human p18^{INK4c} sequence (residues 2–168). $HMTD_{103}$p18, HTatp18, Hphp18, and HAntp18, are identical to Hp18 but contain the hydrophobic MTD103 sequence or protein transduction domains from HIV-I Tat

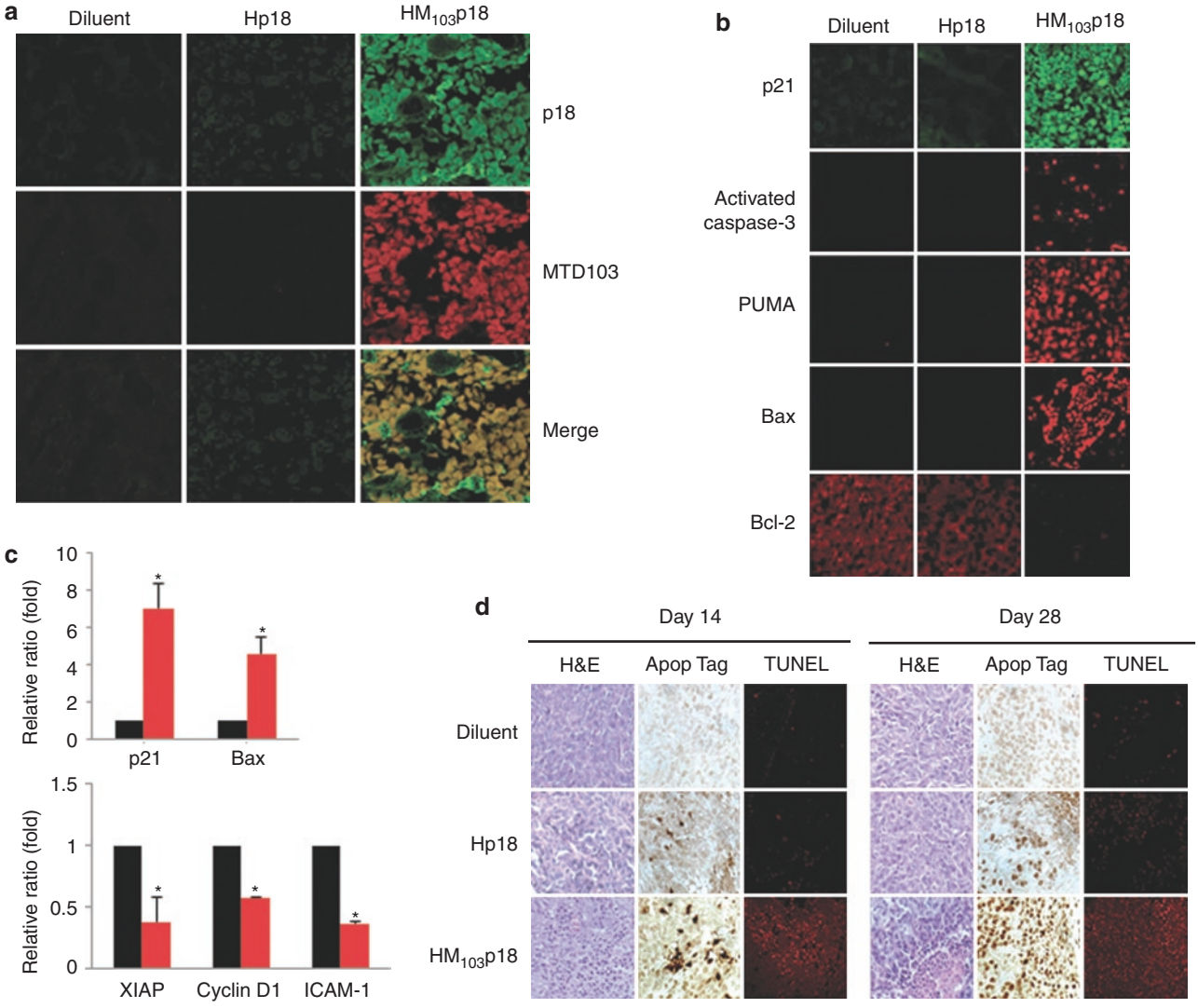

Figure 6 Cell-permeable p18^{INK4c} induces tumor cell apoptosis. (**a**) HM_{103}p18 uptake by HCT116 tumor xenografts. Tumor sections from mice treated daily for 2 weeks with diluent alone, or with 300 µg of either Hp18 or HM_{103}p18 were sectioned and immunostained with antibodies against p18^{INK4c} or MTD103. (**b**,**c**) HM_{103}p18-induced changes in biomarker expression in tumor xenografts, as assessed by (**b**) immunostaining or (**c**) reverse transcriptase PCR. Tumor-bearing mice were prepared and treated as before prior to analysis. Levels of p21, Caspase-3, PUMA, and Bax increased in HM_{103}p18-treated tumors, while levels of Bcl2, XIAP, Cyclin D1, and ICAM-1 declined. Relative expression levels as determined by RT-PCR were averaged from three tumors ± SD. *Significant differences ($P < 0.05$) between HM_{103}p18 and diluent control as determined by one-tailed Student's *t*-tests. (**d**) Cell-permeable p18^{INK4c} induces tumor cell apoptosis. Sections from paraffin-imbedded tumors were prepared after treatment for 14 days and 7 days after protein therapy ended (day 28), and apoptotic cells were visualized by Apop Tag and TUNNEL staining. MTD, macromolecule transduction domain.

(YGRKKRRQRRR), human Hph-1 (YARVRRRGPRR) and *Drosophila* Ant (RQIKIWFQNRRMKWKK), respectively (**Supplementary Tables S2** and **S3**).

The recombinant proteins were purified from *Escherichia coli* BL21-CodonPlus (DE3) cells grown to an A600 of 0.6 and induced for 3 hours with 0.6 mmol/l IPTG. Denatured recombinant proteins were purified by $Ni2^+$ affinity chromatography as directed by the supplier (Qiagen, Hilden, Germany). After purification, they were dialyzed against a refolding buffer (0.55 mol/l guanidine HCl, 0.44 mol/l L-arginine, 50 mmol/l Tris–HCl, 150 mmol/l NaCl, 1 mmol/l EDTA, 100 mmol/l NDSB, 2 mmol/l reduced glutathione, and 0.2 mmol/l oxidized glutathione) and changed to a physiological buffer such as RPMI 1640 medium. The CKI activity of purified Hp18 and HM_{103}p18 proteins was determined by measuring the inhibition of Rb phosphorylation by CDK6/Cyclin D1 kinase, according to the manufacturer's instructions (Cell Signaling, Danvers, MA). The structures of MTD- and PTD-containing p18^{INK4c} proteins were modeled using the AMBER 10.0[35,36] package on a KIST supercomputer based on a continuum solvation model.[37] The relative content of helix, sheet, and coil conformations was calculated using the ptraj program.[35]

Uptake and biological activity of p18^{INK4c} proteins. Recombinant proteins were conjugated to 5/6-FITC, according to the manufacturer's instructions (Pierce Chemical, Rockford, IL). RAW264.7 cells were treated with 10 µmol/l FITC-labeled proteins for 1 hour at 37 °C, washed three times with cold phosphate-buffered saline, treated with proteinase K (10 µg/ml for 20 minutes at 37 °C) to remove cell-surface bound proteins and analyzed by flow cytometry (FACSCalibur; BD Bioscience, Franklin Lakes, NJ). To visualize protein uptake the RAW264.7 cells were exposed to 10 µmol/l FITC-proteins for 1 hour and then nuclei or plasma membranes were counter stained with 1 µg/ml propidium iodide (Sigma-Aldrich, St Louis,

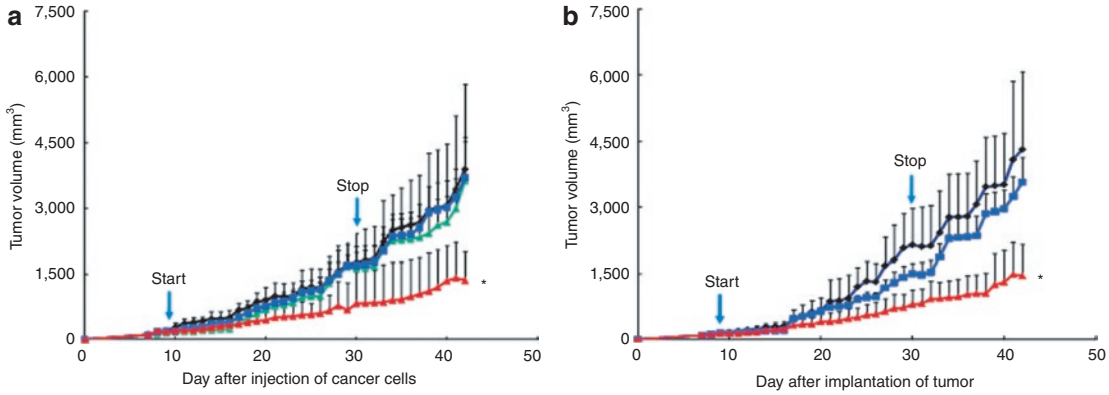

Figure 7 Cell-permeable p18^{INK4c} suppresses the growth of larger tumors. (**a**,**b**) Suppression of tumors induced by subcutaneous injection of (**a**) HCT116 tumor cells or (**b**) HCT116 tumor explants. After tumors reached a size of ~120 mm^3 (start), the mice were injected daily (i.v.) for 3 weeks with diluent alone (black) or with 300 µg Hp18 (blue), HM_{103}p18 (red) or HM_{103}E (green).

MO) or 5 µg/ml FM4-64 (Molecular Probes, Grand Island, NY), respectively and examined by confocal laser scanning microscopy.

HCT116 human colorectal cancer cells (ATCC, Manassas, VA) were maintained as recommended by the supplier. The biologic activity of the cell line was authenticated by *in vivo* tumor growth in Balb/c nu/nu mice. The cell lines were negative for mycoplasma assessed by MycoALERT (2009; Lonza, Basel, Switzerland). The cells were treated with 10 or 20 µmol/l of recombinant proteins for 1 hour. Western blot analyses were performed using antibodies against phospho-Rb (Ser780), Cyclin D1 (92G2), phospho-ATM (Ser1981), p21$^{Waf1/Cip1}$(12D1), phospho-p53 (Ser15) (all from Cell Signaling). β-Actin and horseradish peroxidase-labeled goat anti-mouse immunoglobulin G were acquired from Santa Cruz Biotechnology (Santa Cruz, CA).

Systemic delivery of p18^{INK4c} proteins. Mice (Balb/c, 6-week old, female) were injected intraperitoneally (300 µg/head) with FITC only or FITC-conjugated proteins. After 2 hours, the liver, kidney, spleen, lung, heart, and brain were isolated, washed and frozen with an OCT compound (Sakura, Alphen aan den Rijn, the Netherlands) on dry ice. Cryosections (14 or 20 µm thickness) were analyzed using a fluorescence microscope (Nikon, Tokyo, Japan). For CP-p18^{INK4c} immunostaining, mice were injected with diluent, Hp18 or MTD- or PTD-fused p18^{INK4c} (intravenous, 600 µg/head). At 3 hours following the injection, the spleen and liver were removed, embedded in paraffin, sectioned at 5 µm and stained with mouse anti-p18^{INK4c} antibody (Santa Cruz Biotechnology) or mouse 6X His tag antibody (Abcam, Cambridge, MA), followed by staining with horseradish peroxidase-conjugated goat anti-mouse secondary antibody (Santa Cruz Biotechnology). Protein transduction in white blood cells was assessed 1, 2, 4, or 8 hours postinjection. After proteinase K treatment (10 µg/ml for 20 minutes at 37 °C), B220$^+$ or CD3$^+$ lymphocytes, CD116$^+$ leukocytes, and Ly6G$^+$ neutrophils were analyzed by flow cytometry. Western blot analysis of plasma and spleen or liver lysates was conducted using rabbit anti-p18^{INK4c} antibody (Abcam) and horseradish peroxidase-conjugated goat anti-rabbit secondary antibody (Santa Cruz Biotechnology).

Q-dot-conjugation was conducted according to the manufacturer's instructions (Invitrogen, Grand Island, NY). Mice (Balb/c, 8-week old, female) were injected intraperitoneally or intravenously with diluent (RPMI 1640) or an equimolar concentration of Q-dot or Q-dot-conjugated recombinant proteins. The emitted light was detected with a multispectral imaging system (Maestro2, CRI).

Mechanism of MTD-mediated intracellular delivery. RAW264.7 cells were pretreated with different agents to assess the effect of various conditions on protein uptake: (i) 5 µg/ml proteinase K for 10 minutes, (ii) 20 µmol/l Taxol for 30 minutes, (iii) 10 µmol/l antimycin in the presence or absence of 1 mmol/l ATP for 2 hours (iv) incubation on ice (or maintained at 37 °C) for 15, 30, or 60 minutes, and (v) 100 mmol/l EDTA for 3 hours. These agents were used at concentrations known to be active in other applications. The cells were then incubated with 10 µmol/l FITC-labeled proteins for 1 hour at 37 °C, were washed three times with ice-cold phosphate-buffered saline, treated with proteinase K (10 µg/ml for 20 minutes at 37 °C) to remove cell-surface bound proteins and analyzed by flow cytometry. To assess cell-to-cell protein transfer, RAW264.7 cells containing FITC-conjugated protein were prepared in the same way and mixed with untreated cells labeled with PreCP-Cy5.5-CD14 antibody for 2 hours. Cell-to-cell protein transfer, resulting in FITC-Cy5.5 double-positive cells, was monitored by flow cytometry. Multilamellar vesicles (MLVs) were kindly provided from Dr Dae-Duk Kim (Seoul National University, Seoul, Korea). The multilamellar vesicles were prepared by the thin film hydration method.[38] The lipid film was hydrated with HEPES buffer and multilamellar vesicles formed spontaneously upon gently agitation. Subsequently, the vesicle solution was frozen in liquid nitrogen for 3 minutes and then thawed in a water bath at 40 °C. This freeze-thaw cycle was repeated five times. The vesicles were treated with 10 µmol/l FITC-labeled proteins for 10 minutes at 37 °C, were treated with 5 µg/ml proteinase K to remove any surface bound protein, and were analyzed with a FACSCalibur.

Xenograft tumor model. Female Balb/c nu/nu mice were subcutaneously inoculated with 1×10^6 HCT116 human colorectal cancer cells or implanted with HCT116 tumor block (1 mm^3) into the left side of the back. Tumor-bearing mice were intravenously administered CP-p18^{INK4c} or control proteins (200 or 300 µg/head) for 14 or 21 days and observed for 2–3 weeks following the termination of the treatment. Tumor size was monitored by measuring the longest (length) and shortest dimensions (width) once a day with a dial caliper, and tumor volume was calculated as width^2 × length × 0.5.

Therapy-induced changes in tumor biomarker expression. Expression of cell cycle and apoptosis biomarkers was assessed by real-time PCR and immunohistochemistry. Following a 3-week protein treatment (intravenous, 300 µg/head), total RNA was extracted from isolated tumor using the Trizol reagent according to the manufacturer's instructions (Invitrogen). Real-time PCR was performed on ABI 7900 HT Sequence Detection System. Paraffin-embedded tumor sections (20 µm) were immunostained using monoclonal antibodies against p21$^{Waf1/Cip1}$ (12D1) and activated Caspase-3 (Asp175), and polyclonal antibodies against Bax, PUMA and Bcl2 (all from Cell Signaling). The secondary antibody was Alexa Fluor-488 or -588 labeled-goat anti-mouse immunoglobulin G (Invitrogen).

Apoptosis assays. Annexin V (BD Bioscience) and Caspase-3 (Clontech, Mountain View, CA) assays were conducted according to the manufacturers' instructions. Apoptosis in hematoxylin and eosin-stained tumor sections was assessed by Apop Tag and TUNEL (Roche, Basel, Switzerland).

Statistical analysis. All experimental data obtained from cultured cells are expressed as means ± SD. For the annexin V and caspase-3 assays, statistical significance was evaluated using a one-tailed Student's *t*-test. For animal studies, paired Student's *t*-test was used for in-house *in vivo* experiment (**Figure 5a**). At professional contracted research organization (CRO; Biotoxtech, Ochang, Korea), one-way analysis of variance was calculated using the SAS Program (v9.1.2; SAS Institute, Cary, NC) and if significant, by Dunnett's test for multiple comparisons at the 1.0 and 5.0% one-tailed significance level. Statistical significance was established at $P < 0.05$.

SUPPLEMENTARY MATERIAL

Figure S1. MTD-mediated protein delivery into cells and tissues.
Figure S2. Structures and expression of cell-permeable p18^{INK4c} proteins.
Figure S3. Uptake of cell-permeable p18^{INK4c}.
Figure S4. Mechanism of MTD103-mediated protein uptake.
Figure S5. Structures and expression of alternative p18^{INK4c} fusion proteins.
Figure S6. DNA content of cells treated with cell-permeable (HM_{103}p18) and non cell-permeable (Hp18) p18^{INK4c} proteins.
Figure S7. *In vivo* delivery of CP-p18^{INK4c} in tissues and tumors.
Figure S8. Body weights of tumor-bearing mice.
Figure S9. Predicted structures of MDT and PTD sequences.
Table S1. MTD sequences with enhanced protein transduction activity.
Table S2. PCR primers used to construct PTD-p18^{INK4c} expression vectors.
Table S3. PCR primers used to construct MTD-p18^{INK4c} expression vectors.

ACKNOWLEDGMENTS

We thank Dr Claude Labrie (University of Quebec, Canada) for providing the human p18^{INK4c} cDNA. We also thank Dr Chris Ko for critical comments, the many young scientists who were involved in the early stage of this study for their technical assistance and Jihye Han for her assistance in preparing the manuscript. This study was supported by grants of the Korean Health Technology R&D Project (A085126 to D.J.) of Ministry of Health & Welfare, and the Industrial Strategic Technology Development Program (10032101 to D.J.) of Ministry of Knowledge Economy, Republic of Korea. D.J. was the founding scientist of ProCell Therapeutics, Inc., and is affiliated to Vanderbilt University at present. J.L., J.K., G.L., J.K., and J.Y. are employees of ProCell Therapeutics, Inc. Hereby; these authors disclose a financial interest in the company. The other authors declared no conflict of interest.

REFERENCES

1. Malumbres, M and Barbacid, M (2009). Cell cycle, CDKs and cancer: a changing paradigm. *Nat Rev Cancer* **9**: 153–166.
2. Sherr, CJ and Roberts, JM (1999). CDK inhibitors: positive and negative regulators of G1-phase progression. *Genes Dev* **13**: 1501–1512.
3. Landis, MW, Pawlyk, BS, Li, T, Sicinski, P and Hinds, PW (2006). Cyclin D1-dependent kinase activity in murine development and mammary tumorigenesis. *Cancer Cell* **9**: 13–22.
4. Yu, Q, Sicinska, E, Geng, Y, Ahnström, M, Zagozdzon, A, Kong, Y *et al.* (2006). Requirement for CDK4 kinase function in breast cancer. *Cancer Cell* **9**: 23–32.
5. Pei, XH, Bai, F, Smith, MD, Usary, J, Fan, C, Pai, SY *et al.* (2009). CDK inhibitor p18(INK4c) is a downstream target of GATA3 and restrains mammary luminal progenitor cell proliferation and tumorigenesis. *Cancer Cell* **15**: 389–401.
6. Reddy, HK, Graña, X, Dhanasekaran, DN, Litvin, J and Reddy, EP (2010). Requirement of Cdk4 for v-Ha-ras-Induced Breast Tumorigenesis and Activation of the v-ras-Induced Senescence Program by the R24C Mutation. *Genes Cancer* **1**: 69–80.
7. Puyol, M, Martín, A, Dubus, P, Mulero, F, Pizcueta, P, Khan, G *et al.* (2010). A synthetic lethal interaction between K-Ras oncogenes and Cdk4 unveils a therapeutic strategy for non-small cell lung carcinoma. *Cancer Cell* **18**: 63–73.
8. Lapenna, S and Giordano, A (2009). Cell cycle kinases as therapeutic targets for cancer. *Nat Rev Drug Discov* **8**: 547–566.
9. Malumbres, M, Pevarello, P, Barbacid, M and Bischoff, JR (2008). CDK inhibitors in cancer therapy: what is next? *Trends Pharmacol Sci* **29**: 16–21.
10. Fischer, PM (2007). Cellular uptake mechanisms and potential therapeutic utility of peptidic cell delivery vectors: progress 2001-2006. *Med Res Rev* **27**: 755–795.
11. Heitz, F, Morris, MC and Divita, G (2009). Twenty years of cell-penetrating peptides: from molecular mechanisms to therapeutics. *Br J Pharmacol* **157**: 195–206.
12. Moore, DJ, Zienkiewicz, J, Kendall, PL, Liu, D, Liu, X, Veach, RA *et al.* (2010). *In vivo* islet protection by a nuclear import inhibitor in a mouse model of type 1 diabetes. *PLoS ONE* **5**: e13235.
13. Jo, D, Liu, D, Yao, S, Collins, RD and Hawiger, J (2005). Intracellular protein therapy with SOCS3 inhibits inflammation and apoptosis. *Nat Med* **11**: 892–898.
14. Liu, D, Li, C, Chen, Y, Burnett, C, Liu, XY, Downs, S *et al.* (2004). Nuclear import of proinflammatory transcription factors is required for massive liver apoptosis induced by bacterial lipopolysaccharide. *J Biol Chem* **279**: 48434–48442.
15. Liu, D, Liu, XY, Robinson, D, Burnett, C, Jackson, C, Seele, L *et al.* (2004). Suppression of Staphylococcal Enterotoxin B-induced Toxicity by a Nuclear Import Inhibitor. *J Biol Chem* **279**: 19239–19246.
16. Liu, D, Zienkiewicz, J, DiGiandomenico, A and Hawiger, J (2009). Suppression of acute lung inflammation by intracellular peptide delivery of a nuclear import inhibitor. *Mol Ther* **17**: 796–802.
17. Liu, XY, Robinson, D, Veach, RA, Liu, D, Timmons, S, Collins, RD *et al.* (2000). Peptide-directed suppression of a pro-inflammatory cytokine response. *J Biol Chem* **275**: 16774–16778.
18. Lim, J, Jang, G, Kang, S, Lee, G, Nga, do TT, Phuong, do TL *et al.* (2011). Cell-permeable NM23 blocks the maintenance and progression of established pulmonary metastasis. *Cancer Res* **71**: 7216–7225.
19. Veach, RA, Liu, D, Yao, S, Chen, Y, Liu, XY, Downs, S *et al.* (2004). Receptor/transporter-independent targeting of functional peptides across the plasma membrane. *J Biol Chem* **279**: 11425–11431.
20. Ramamoorthy, A, Kandasamy, SK, Lee, DK, Kidambi, S and Larson, RG (2007). Structure, topology, and tilt of cell-signaling peptides containing nuclear localization sequences in membrane bilayers determined by solid-state NMR and molecular dynamics simulation studies. *Biochemistry* **46**: 965–975.
21. Lin, Q, Jo, D, Gebre-Amlak, KD and Ruley, HE (2004). Enhanced cell-permeant Cre protein for site-specific recombination in cultured cells. *BMC Biotechnol* **4**: 25.
22. Sung, M, Poon, GM and Gariépy, J (2006). The importance of valency in enhancing the import and cell routing potential of protein transduction domain-containing molecules. *Biochim Biophys Acta* **1758**: 355–363.
23. Guan, KL, Jenkins, CW, Li, Y, Nichols, MA, Wu, X, O'Keefe, CL *et al.* (1994). Growth suppression by p18, a p16INK4/MTS1- and p14INK4B/MTS2-related CDK6 inhibitor, correlates with wild-type pRb function. *Genes Dev* **8**: 2939–2952.
24. Ball, KL, Lain, S, Fâhraeus, R, Smythe, C and Lane, DP (1997). Cell-cycle arrest and inhibition of Cdk4 activity by small peptides based on the carboxy-terminal domain of p21WAF1. *Curr Biol* **7**: 71–80.
25. Bonfanti, M, Taverna, S, Salmona, M, D'Incalci, M and Broggini, M (1997). p21WAF1-derived peptides linked to an internalization peptide inhibit human cancer cell growth. *Cancer Res* **57**: 1442–1446.
26. Chen, QR, Kumar, D, Stass, SA and Mixson, AJ (1999). Liposomes complexed to plasmids encoding angiostatin and endostatin inhibit breast cancer in nude mice. *Cancer Res* **59**: 3308–3312.
27. Ezhevsky, SA, Ho, A, Becker-Hapak, M, Davis, PK and Dowdy, SF (2001). Differential regulation of retinoblastoma tumor suppressor protein by G(1) cyclin-dependent kinase complexes in vivo. *Mol Cell Biol* **21**: 4773–4784.
28. Gius, DR, Ezhevsky, SA, Becker-Hapak, M, Nagahara, H, Wei, MC and Dowdy, SF (1999). Transduced p16INK4a peptides inhibit hypophosphorylation of the retinoblastoma protein and cell cycle progression prior to activation of Cdk2 complexes in late G1. *Cancer Res* **59**: 2577–2580.
29. Nagahara, H, Vocero-Akbani, AM, Snyder, EL, Ho, A, Latham, DG, Lissy, NA *et al.* (1998). Transduction of full-length TAT fusion proteins into mammalian cells: TAT-p27Kip1 induces cell migration. *Nat Med* **4**: 1449–1452.
30. Aderibigbe, OR, Pisa, PT, Mamabolo, RL, Kruger, HS and Vorster, HH (2011). The relationship between indices of iron status and selected anthropometric cardiovascular disease risk markers in an African population: the THUSA study. *Cardiovasc J Afr* **22**: 249–256.
31. Kraeft, SK, Traincart, F, Mesnildrey, S, Bourdais, J, Véron, M and Chen, LB (1996). Nuclear localization of nucleoside diphosphate kinase type B (nm23-H2) in cultured cells. *Exp Cell Res* **227**: 63–69.
32. Fry, DW, Harvey, PJ, Keller, PR, Elliott, WL, Meade, M, Trachet, E *et al.* (2004). Specific inhibition of cyclin-dependent kinase 4/6 by PD 0332991 and associated antitumor activity in human tumor xenografts. *Mol Cancer Ther* **3**: 1427–1438.
33. Noh, SJ, Li, Y, Xiong, Y and Guan, KL (1999). Identification of functional elements of p18INK4C essential for binding and inhibition of cyclin-dependent kinase (CDK) 4 and CDK6. *Cancer Res* **59**: 558–564.
34. Li, J, Poi, MJ, Qin, D, Selby, TL, Byeon, IJ and Tsai, MD (2000). Tumor suppressor INK4: quantitative structure-function analyses of p18INK4C as an inhibitor of cyclin-dependent kinase 4. *Biochemistry* **39**: 649–657.
35. Kabsch, W and Sander, C (1983). Dictionary of protein secondary structure: pattern recognition of hydrogen-bonded and geometrical features. *Biopolymers* **22**: 2577–2637.
36. Case, DA, Darden, TA, Cheatham, ITE, Simmerling, CL, Wang, J, Duke, RE *et al. AMBER 10*. University of California San Francisco: San Francisco, 2008.
37. Sigalov, G, Scheffel, P and Onufriev, A (2005). Incorporating variable dielectric environments into the generalized Born model. *J Chem Phys* **122**: 094511.
38. Mayer, LD, Hope, MJ, Cullis, PR and Janoff, AS (1985). Solute distributions and trapping efficiencies observed in freeze-thawed multilamellar vesicles. *Biochim Biophys Acta* **817**: 193–196.